Lasers in Surgery and Medicine 27:191–205 (2000)

Optic Nerve Sheath Fenestration With a Novel Wavelength Produced by the Free Electron Laser (FEL)

Karen M. Joos, MD, PhD,[1]* Jin H. Shen, PhD,[1] Debra J. Shetlar, MD, PhD,[1–3] and Vivien A. Casagrande, PhD[1,4]

[1]*Department of Ophthalmology and Visual Sciences, Vanderbilt University, Nashville, Tennessee*
[2]*Department of Pathology, Vanderbilt University, Nashville, Tennessee*
[3]*Cullen Eye Institute, Baylor College of Medicine, Houston, Texas*
[4]*Departments of Cell Biology and Psychology, Vanderbilt University, Nashville, Tennessee*

Background and Objective: **To determine whether 6.45-μm free electron laser (FEL) energy can successfully perform optic nerve sheath fenestration and to compare the acute and chronic cellular responses with this surgery.**
Study Design/Materials and Methods: **Optic nerve sheath fenestration was performed in rabbits by using either FEL energy (< 2.5 mJ, 10 Hz, 325-μm spot size) or a knife. The optic nerve integrity and glial response were evaluated histologically acutely or 1 month postoperatively.**
Results: **The FEL at low energy effectively cut the optic nerve sheaths with minimal reaction in the underlying nerve. With FEL or knife surgical techniques, a mild astrocytic hypertrophy only adjacent to the fenestration was observed acutely in the glial fibrillary acidic protein (GFAP) -immunoreacted sections. The chronic healing responses after either technique appeared similar with: (1) a thin fibrous scar at the fenestration site, (2) cells uniformly distributed (hematoxylin and eosin), and (3) up-regulation of GFAP and S100β in astrocytes adjacent to the fenestration site.**
Conclusion: **The FEL at low energy performs an optic nerve sheath fenestration in a small space with ease. Both FEL and knife incisions cause a similar rapid glial response near the fenestration site that remains 1 month later. Lasers Surg. Med. 27:191–205, 2000.**

Key words: glial cell; immunocytochemistry; laser; optic nerve; optic nerve sheath fenestration; surgery; papilledema

INTRODUCTION

Pseudotumor cerebri is characterized by headaches, visual obscurations, marked vision loss, deterioration of the visual field, and optic disc swelling. In adults, the course can be more protracted with associations including obesity, middle ear disease, pregnancy, corticosteroid use or withdrawal, high-dose vitamin A, nalidixic acid, tetracycline, nutrition disorders, toxins, immune disorders, or after mild head trauma [1,2]. Increased intracranial pressure also can occur secondary to cerebral venous outflow obstruction [3,4]. The increased pressure causes headaches and is transmitted along the subarachnoid space of the optic nerve to produce papilledema of the optic disc [5]. Treatment is aimed at decreasing the intracranial pressure around the optic nerves.

Contract grant sponsor: Department of Defense Medical Free Electron Laser Program, Office of Naval Research; Contract grant number: N00014-94-1-1023; Contract grant sponsor: Research to Prevent Blindness, Inc.; Contract grant sponsor: National Institutes of Health; Contract grant number: Core Grant EY08126.

*Correspondence to: Karen Joos, MD, PhD, Department of Ophthalmology and Visual Sciences, 1215 21st Avenue South, 8017 MCE, Nashville, TN 37232-8808.
E-mail: karen.joos@mcmail.vanderbilt.edu

Accepted 17 March 2000

Surgical treatments are performed when medical therapies fail to prevent vision loss or are not tolerated by the patient [6].

Optic nerve sheath decompression has been successful in preventing and even restoring lost vision [7,8]. However, it can be technically difficult to expose and then cut a window or incise multiple slits typically with a knife or scissors in the sheath without disturbing the underlying optic nerve. Also, approximately 30% of the successful procedures may fail within 5 years with visual deterioration [8]. If pseudotumor cerebri is not successfully treated, gliosis of the optic nerve head may cause permanent severe vision loss or visual field loss [7]. Even with treatment, partial loss of vision may occur in some patients. Histologic loss of parvocellular and magnocellular cells in the lateral geniculate nucleus has been observed in pathologic specimens [9].

Improvements in the surgical technique have been investigated, including approaching the optic nerve medially instead of removing bone laterally and exploring adjunctive use of mitomycin C or by using small shunts around the optic nerve [10,11]. Our preliminary data on cadaver tissue suggested that a 6.45-μm wavelength with a 325-μm spot size at 10 Hz produced by the Vanderbilt University free electron laser (FEL) might incise the meningeal sheath without damaging the underlying optic nerve. No thermal damage to the optic nerve was evident in this histologic study [12]. One group found thermal damage at the optic nerve with a contact Nd:YAG laser but not with noncontact Nd:YAG or CO_2 lasers aimed at adjacent muscle in pigs [13]. These investigators were not attempting to perform optic nerve sheath fenestration. The FEL is an infrared research laser that is tunable between 2 and 9 μm with a 4-μsec macropulse structure consisting of a train of picosecond pulses spaced 350 psec apart. Therefore, wavelengths corresponding to specific molecular absorption peaks may be selected for investigation.

FEL energy tuned at specific wavelengths has produced minimal collateral damage in some neural and ocular tissues [12,14]. The usefulness of the Amide II (C-N-H absorption peak) band 6.45 μm as an incising wavelength with minimal collateral damage was demonstrated in brain tissue [14]. Besides successfully incising cadaver meningeal sheaths without underlying optic nerve thermal damage at the Amide II wavelength (6.45 μm), incisions with minimal collateral thermal damage were produced at the Amide I band (6.0 μm) for cadaver corneal tissue; and at 6.0 μm, 6.1 μm (a water absorption peak), or 6.45 μm for cadaver retinal tissue [12]. These data suggested that the FEL might have a significant advantage in investigating potential improvements in ocular surgery. This opportunity was possible because glass-hollow waveguides could be incorporated into a customized sterilized surgical handpiece with 18- to 20-gauge tips for precise delivery of the laser energy to small ocular structures [15].

The primary purpose of this study was to determine whether this FEL Amide II wavelength of 6.45 μm [14] is capable of precisely incising the optic nerve sheath and to compare the histologic healing responses with those produced by traditional mechanical incisions. A second related objective was to understand more about the cell biological response to surgical manipulation of the optic nerve and to the acute and chronic removal of a portion of the meningeal sheath. Investigators have used MRI to examine optic nerve sheath fenestrations postoperatively [16], but there have been no systematic immunocytochemical studies of the structural changes and glial responses after optic nerve sheath fenestration.

METHODS

Animals

Adult Dutch Belted rabbits weighing an average of 2.3 kg were used in this study. All animal procedures were performed in accordance with National Institutes of Health and Department of Defense guidelines and with approval of the Vanderbilt Institutional Animal Care and Use Committee. Rabbits received optic nerve sheath fenestrations with the free electron laser (FEL) ($n = 6$) or with a knife ($n = 2$). Controls involved either a sham surgery ($n = 5$) or no surgery ($n = 3$). These rabbits survived for 1 month before killing during which time their optic nerve heads and retinas were examined at weekly intervals. Other rabbits received acute optic nerve sheath fenestrations with the FEL ($n = 4$) or knife ($n = 4$) and were killed immediately after surgery.

Surgical Procedures

Anesthesia was induced with intramuscular (IM) injections of a mixture of ketamine 35 mg/kg, xylazine 5 mg/kg, and acepromazine 0.75 mg/kg with supplemental half-doses given as needed to maintain anesthesia. During surgery, the ani-

mals were kept warm and were continuously monitored. Under sterile surgical conditions, the eyelids were retracted after making a lateral canthotomy. Proparacaine drops were instilled in the eye, and a superior conjunctival peritomy was performed. A 6-0 Vicryl suture was passed through the superior rectus muscle, and this muscle was disinserted. After extensive retraction the optic nerve could be observed. All eyes except unoperated controls were treated with the surgical steps described above. The surgery was terminated at this point in the sham controls. An ophthalmic operating microscope was used to visualize the optic nerve sheath and the optic nerve during all procedures. In 15 experimental eyes, a 2-mm-diameter window was produced by incising the optic nerve sheath either with a 15 degree knife or with FEL energy (6.45 μm, 10 Hz, < 2.5 mJ, 325-μm spot size, 5-μsec macropulse) by using a 530-μm diameter hollow waveguide probe. Energy levels were determined by using an energy meter (Molectron Detector, Inc., Portland, OR) just before and immediately after lasing. On the optic nerve sheath of one experimental eye, three times the cutting energy (7.5 mJ) was used to evaluate the tissue response. The FEL hollow waveguide delivery system was constructed specifically for these surgical procedures [15]. With this system, the FEL beam was transmitted through nitrogen-purged pipes to the hollow waveguide connector. The hollow waveguide was enclosed within a narrow sterilized surgical probe designed to be hand held and easy to maneuver. The FEL probe was held approximately 1–2 mm from the optic nerve sheath surface. After a circular incision was made in the meninges with either the FEL or the knife, a Sinsky hook was used to carefully lift and remove the dura and arachnoid to create the fenestration window. The superior rectus muscle was then reattached. The conjunctiva and the lateral canthotomy were repaired. The survival rabbits were given Yohimbine 0.2 mg/kg and Ketoprofen 1 mg/kg IM. The rabbits that received acute procedures were killed without awakening from surgery.

Ocular Examinations

The survival rabbits were examined weekly with an indirect ophthalmoscope, and the optic nerve head was photographed and its condition documented.

Histology and Immunocytochemistry

The rabbits were given a lethal overdose of anesthetic and were perfused transcardially first with PBS followed by 3% formaldehyde, 0.1% glutaraldehyde (v/v), and 0.2% saturated picric acid (v/v), in 0.1 M phosphate buffer. Eyes with optic nerves attached were removed and placed in the same fixative overnight. The eyes/nerves then were dissected into two components. One component contained a portion of the retina, optic nerve head, and the segment of optic nerve in which the fenestration had been performed. This component was sectioned from superior to inferior. Because the fenestration was made close to the globe where the rabbit optic nerve adheres to the globe, this plane of cut allowed us to identify easily the location of the fenestration in sections. The other component contained the proximal segment of optic nerve and was cut in cross-section.

The dissected tissue then was dehydrated, embedded in paraffin, and sectioned at 5–10 μm. Selected sections were deparaffinized and stained with hematoxylin and eosin (H&E). Serial sections were examined to determine the exact location of the optic nerve sheath fenestration. Sections through this region then were stained with H&E or immunoreacted for antibodies to glial fibrillary acidic protein (GFAP) and S100β in series. Comparable regions of optic nerve in all sham or normal controls also were stained or immunoreacted in the same way.

For immunocytochemistry, the deparaffinized sections were placed into 100% methanol with 0.3% hydrogen peroxide (H_2O_2) to block endogenous peroxidase and then were rehydrated and placed into 4% normal goat serum and 0.1% Triton X in Tris buffered saline (TBS). Primary and secondary antibodies were prepared in TBS with 0.2% Triton-X 100 and 2% normal horse serum. A dilution series was run to determine the best concentration of primary monoclonal antibodies to use for this tissue. S100β (S-2532, Sigma, St. Louis, MO) was used at 1:1,000, GFAP (814-369, Boehringer Mannheim, Indianapolis, IN) was used at 1:500. Negative controls were performed by omitting primary antibodies on some sections in all nerves. No staining was observed in control sections. The primary antibodies were left on the sections overnight, followed by three rinses in TBS, and then placed in biotinylated horse anti-mouse (BA-2000, Vector, Burlingame, CA) at 1:200 for 2 hours. Sections were rinsed 3× in TBS and placed in ABC Standard Elite (PK-6100,Vector) used at half the recommended strength for 2 hours, then rinsed 3× in TBS. Sections were incubated in 0.5% diaminobenzidine (D-5637, Sigma) in TBS with 0.04%

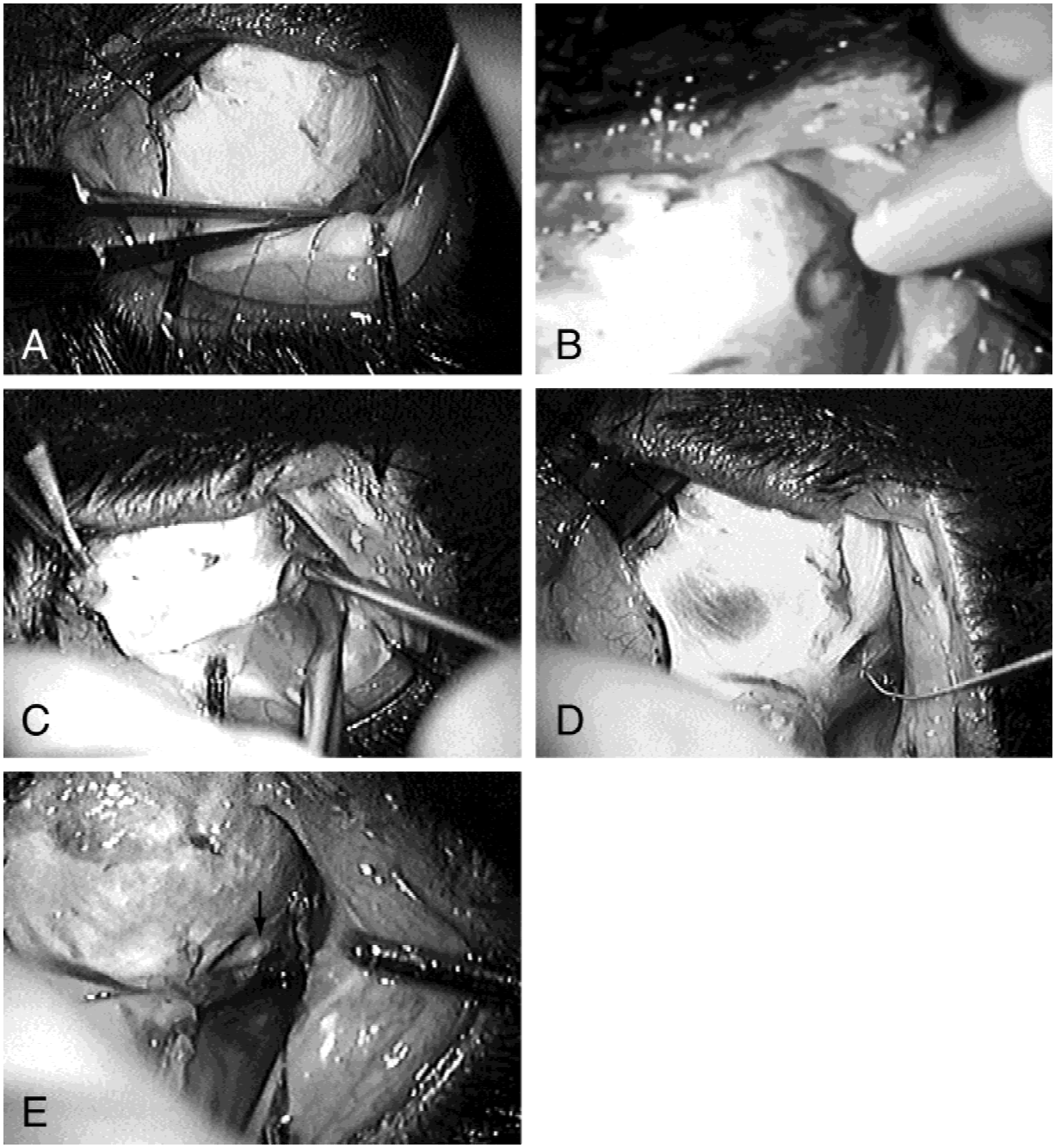

Fig. 1. **A:** The superior rectus muscle is disinserted and retracted to expose the distal optic nerve sheath in the rabbit. **B:** A 15-degree knife is used to incise the optic nerve sheath. **C:** A sterile hollow waveguide probe delivers the free electron laser (FEL) energy to the optic nerve sheath. **D:** A Sinsky hook is used to lift the incised dura and arachnoid layers. **E:** A window over the optic nerve is visible after removal of the incised sheath (arrow).

nickel ammonium sulfate for 15 minutes and then reacted in the same diaminobenzidine solution with 0.006% H_2O_2 added.

RESULTS

Surgical Procedure

Sufficient exposure of the optic nerve was obtained in all cases. Once the nerve was exposed (Fig. 1A), maneuverability with the FEL probe was found to be technically easier in the small space compared with maneuverability with the knife. Release of cerebral spinal fluid (CSF) along the cut edge of the meninges was taken as the initial sign that either the laser or knife cut (Fig. 1B) was deep enough. Figure 1C shows the waveguide probe delivering the FEL laser energy

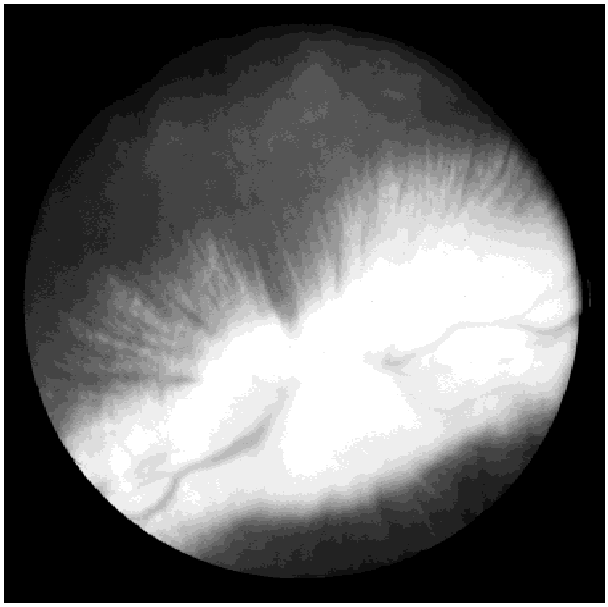

Fig. 2. Ophthalmoscopic examination of the fundus demonstrated no change after free electron laser optic nerve sheath fenestration. This photograph was taken 3 weeks after surgery.

to the optic nerve sheath. By using the FEL probe viewed under the surgical microscope, it was relatively easy and efficient to cut along the circumference of a 2-mm diameter circle and then use the Sinsky hook (Fig. 1D) to lift the dura and arachnoid away from the underlying optic nerve fibers. For most rabbit nerves, one pass of the laser at an average of 2.0 mJ was sufficient to cut the meninges. Rarely, two passes were required. Several small cuts with the knife were required within the small retrobulbar space to achieve the same result achieved in less time with the laser probe. Initially, a higher energy level of 7.5 mJ (more than 3 times that required to incise the meninges) was tried. This energy was observed to incise too deeply and damage the underlying nerve, a result that was later confirmed histologically (see below).

Postsurgical Ocular Examinations

No postoperative complications occurred in any of the rabbits. No fundus abnormalities were noted on weekly indirect ophthalmoscopic examinations. Figure 2 shows an example of a fundus photograph of one rabbit taken 3 weeks after optic nerve sheath fenestration using the FEL. Even in the case where 7.5 mJ caused histologically verified damage to the optic nerve, the retina and optic nerve head appeared healthy by ophthalmoscopy and not different from normal.

Histology and Immunocytochemistry: Controls

Two types of controls were used in these experiments. In three eyes, no surgery was performed, and, in 5 eyes, a sham operation was performed. Both controls survived for 1 month. In unoperated controls, glial nuclei showed an even distribution within the nerve with H&E stain, and the meninges exhibited a normal laminar appearance at the edge of the nerve (Fig. 3A). Astrocytes labeled with either GFAP (Fig. 3B,D) or S100β (Fig. 3C) were relatively evenly distributed throughout the nerve. In contrast to the normal nerves, all of the sham-operated control nerves exhibited a mild astroglial hypertrophy with fine glial processes at the edge of the nerve which was exposed during the sham surgery (Fig. 4B,D). This reaction was only evident in astrocytes in the sections reacted for GFAP (Fig. 4B,D) but not in those stained for H&E to reveal all glia (Fig. 4A) or S100β to show the distribution of astrocytes containing this calcium binding protein (Fig. 4C). We also believe this was not an edge artifact, because it was consistently located in the region where the nerve was exposed in all five sham cases, a result not seen in unoperated controls. This result suggests that the glial reaction seen in the sham nerves was a reflection not of glial proliferation, per se, but a change in the distribution or number of intermediate filaments within the astrocytic processes at the edge of the nerve simply in response to the minimal mechanical manipulation.

Histology and Immunocytochemistry: Acute Surgery

Sections of the optic nerves through the sites of the fenestrations produced acutely with the knife and with the FEL at 6.45 μm and < 2.5 mJ are shown in Figures 5 and 6, respectively. Both the knife and the laser were effective in cutting the sheath without incising the underlying nerve. The cut edge of the sheath is shown toward the top of each photomicrograph in subsequent figures. Arrows in Figures 5A (knife) and 6A (laser) showing H&E-stained sections indicate edges of the cut sheath. The distribution of glia and supporting cells within the nerve revealed in H&E sections was even after acute fenestration with either the knife (Fig. 5B) or the laser (Fig. 6B), indicating that glia did not divide within the 1- to 2-hour period after surgery. However, even during this short period, a mild hypertrophy of astrocytes is evident after either the acute knife or la-

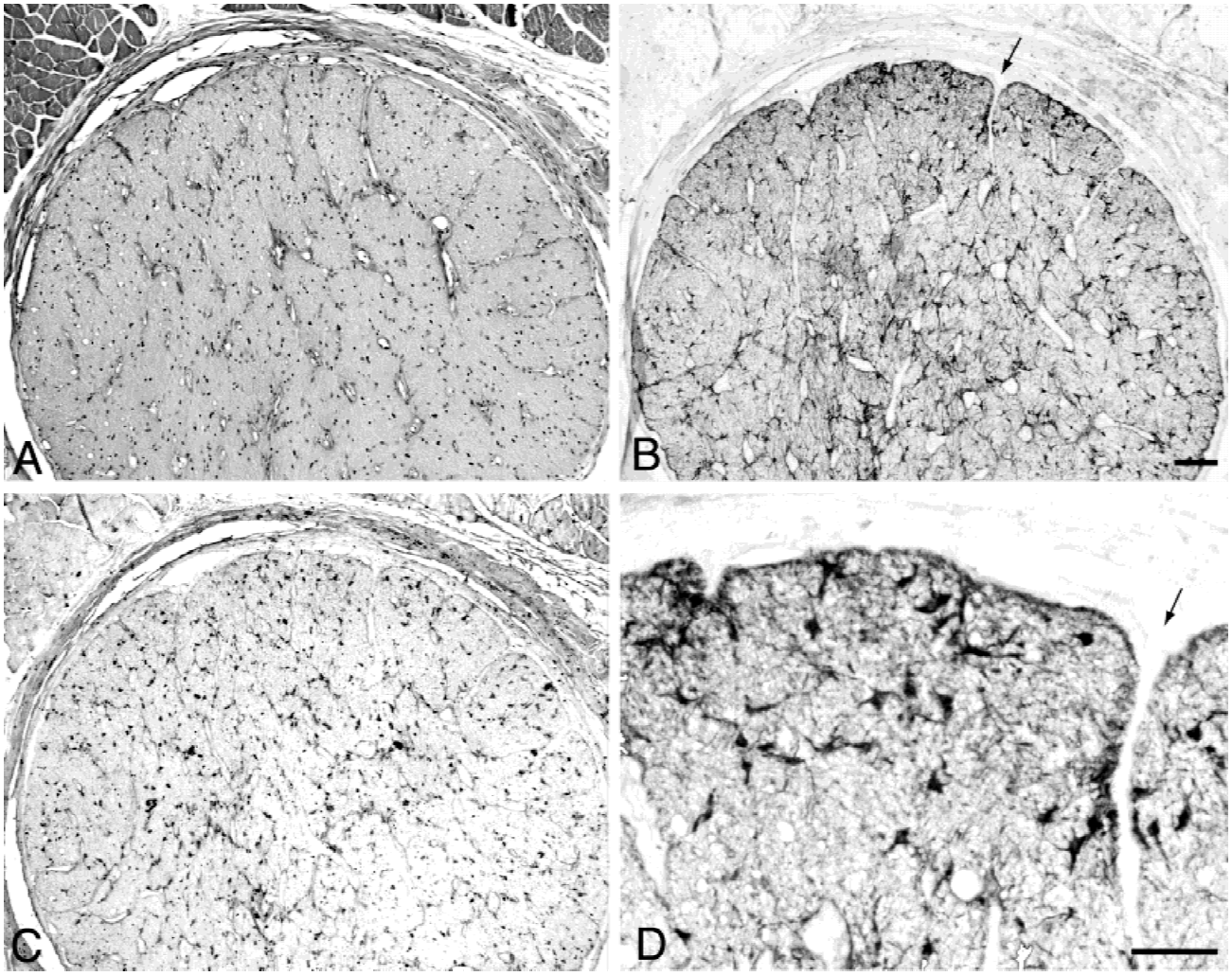

Fig. 3. An unoperated control is cross-sectioned to demonstrate the normal distal optic nerve and overlying sheath histology. **A:** Glial nuclei showed an even distribution within the nerve in an hematoxylin and eosin stain, and the meninges exhibited a normal laminar appearance at the edge of the nerve. **B:** Glial fibrillary acidic protein–labeled astrocytes were evenly distributed. The arrow indicates the same location as in D. **C:** Astrocytes labeled with S100β were evenly distributed throughout the nerve. **D:** Higher magnification photomicrograph of B. Scale bars = 100 μm in B (applies to A–C); 50 μm in D.

ser fenestration as can be seen in the GFAP-immunoreacted sections shown in Figure 5C,D for the knife and in Figure 6C,D for the FEL. This glial reaction was limited to a zone adjacent to the fenestration and was seen after either treatment. The variation in glial hypertrophy seen in the acute fenestration cases with GFAP was within the range of that seen after 1-month survival (see below). There was no evidence of a change in the distribution of astrocytes labeled with S100β after acute fenestration with either the knife (Fig. 5E,F) or the FEL (Fig. 6E,F).

Histology and Immunocytochemistry: Chronic Surgery

Damage to the optic nerve only occurred with the FEL at an excessive energy level (7.5 mJ) as can be seen in Figure 7 for a rabbit that survived for 1 month after the FEL fenestration. In this case, thermal damage was clearly evident in the H&E-stained sections through the level of the fenestration (Fig. 7A,B). As can be seen in Figure 7B, fibrous scar tissue covered the damaged portion of the nerve and some fibroblasts appeared to invade the edge of the nerve itself. GFAP-positive astrocytes showed marked hypertrophy immediately adjacent to the fenestration (Fig. 7C,D) and appeared hypertrophied through the full thickness of the nerve (Fig. 7D). Astrocytes immunolabeled with S100β were not evident immediately adjacent to the site of the fenestration in this case but were present in neighboring areas (Fig. 7E,F) where S100β appeared to be up-regulated in some cells in comparison to control cells (Figs. 3C, 4C).

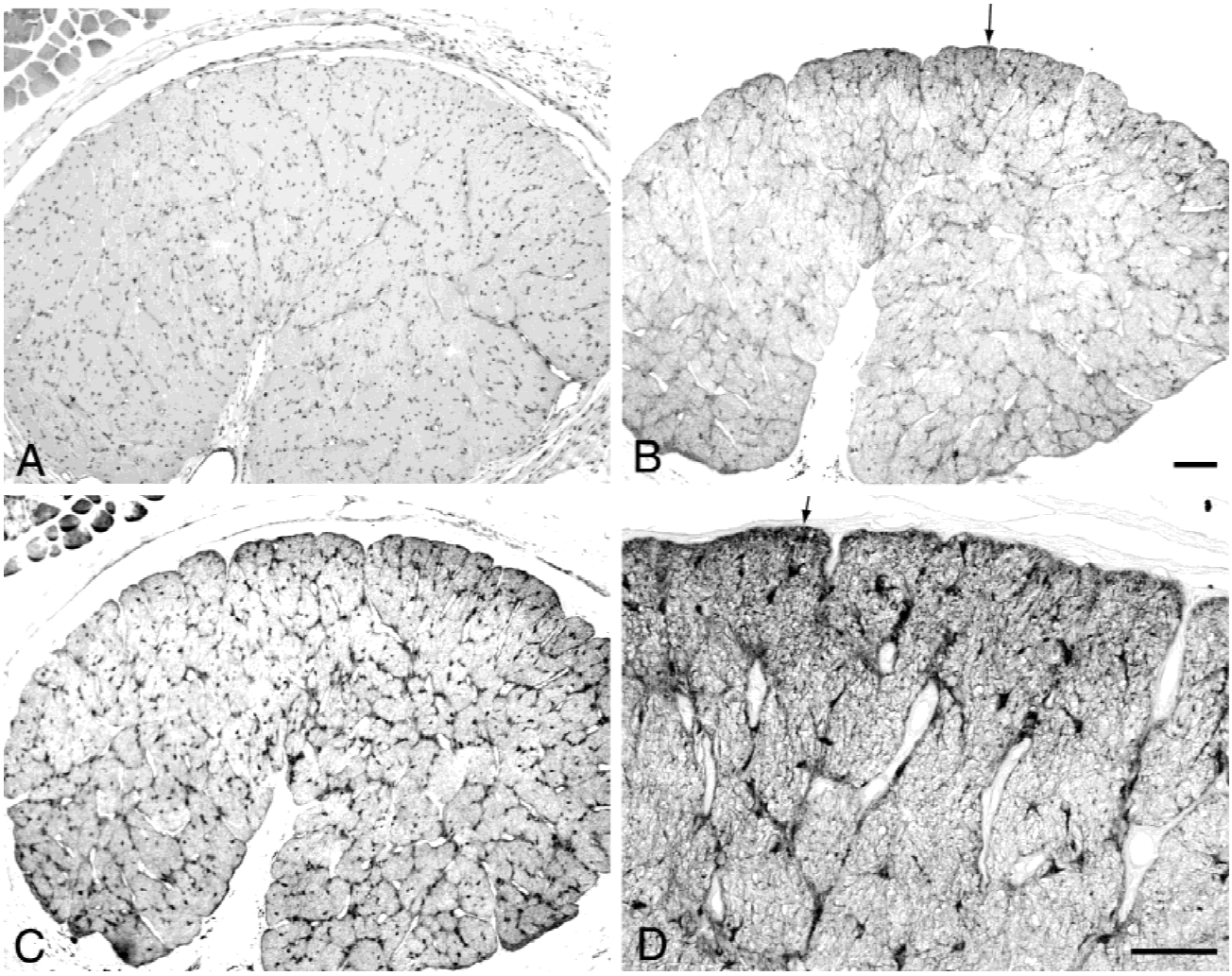

Fig. 4. A sham surgical control is cross-sectioned 1 month postoperatively to demonstrate the normal distal optic nerve and overlying sheath histology. **A:** Glial nuclei showed an even distribution within the nerve in a hematoxylin and eosin stain, and the meninges exhibited a normal laminar appearance at the edge of the nerve. **B:** All of the sham-operated control nerves exhibited mild glial fibrillary acidic protein (GFAP) -positive astroglial hypertrophy at the edge of the nerve that was uncovered during the sham surgery (arrow). This reaction was only evident in astrocytes in the sections reacted for GFAP. **C:** Astrocytes labeled with S100β were evenly distributed throughout the nerve. **D:** Higher magnification photomicrograph of B. Scale bars = 100 μm in B (applies to A–C); 50 μm in D.

In all other chronic cases, the healing response after the knife incisions (Fig. 8) and the < 2.5 mJ FEL incisions (Fig. 9) appeared quite similar. In H&E-stained sections, a thin fibrous scar with granulation was evident at the level of the fenestration completely covering the original opening and extending into the subarachnoid space (Figs. 8A,B, 9A,B).

In H&E-stained sections, glial and supporting cells were evenly distributed. However, both with the knife (Fig. 8C,D) and with the FEL (Fig. 9C,D) fenestrations, astrocytes appeared hypertrophied in all GFAP-immunostained sections adjacent to the original site of the fenestration. Unlike in the acute fenestration cases, in the chronic cases, we did see evidence of up-regulation of S100β in glia close to the site of the original fenestration (Figs. 8E,F, 9E,F). It is not clear whether up-regulation of intermediate filaments (GFAP) occurs in the same glial cells as up-regulation of the calcium binding protein (S100β). The distributions appeared to differ somewhat, suggesting that these responses may involve different populations of astrocytes.

DISCUSSION

Our chief finding is that the FEL with parameters of 6.45-μm, < 2.5 mJ, 10 Hz, 5-μsec

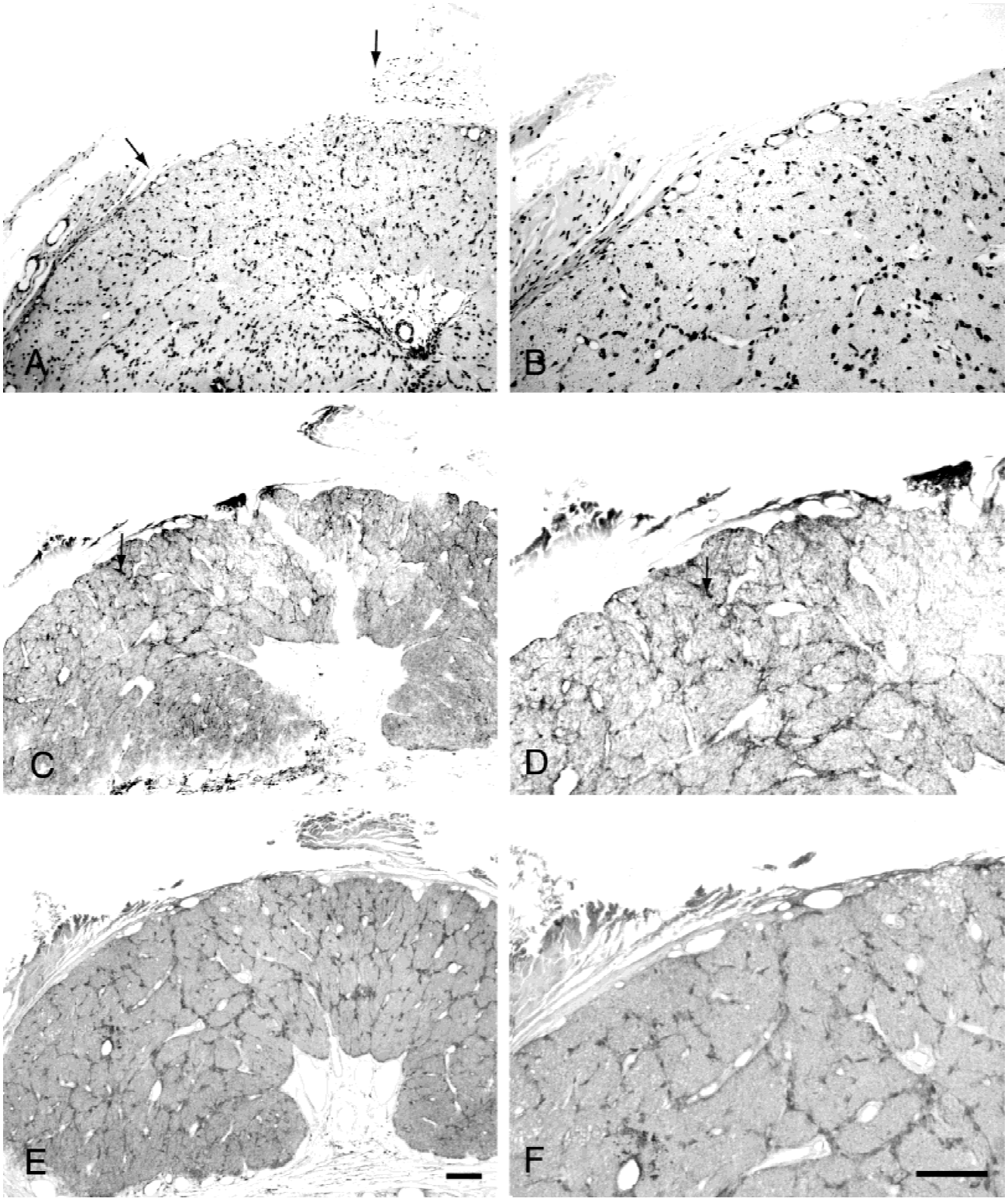

Fig. 5. Illustrated are sections of the optic nerve through the level of the fenestrations produced acutely with the knife. The knife was effective in cutting the sheath without damaging the underlying nerve. B, D, and F show higher magnification photomicrographs of sections illustrated in A, C, and E, respectively, in this and all subsequent figures. **A:** Edges of the cut sheath were easily observed (arrows, hematoxylin and eosin [H&E]). **B:** Distributions of glia and supporting cells within the nerve were uniform after acute fenestration with the knife (H&E). **C:** A mild hypertrophy of astrocytes was evident after the acute knife fenestration in glial fibrillary acidic protein (GFAP) -immunoreacted sections but was limited to a zone adjacent to the fenestration (arrow). Note that the gap in the section is a histologic artifact. **D:** Mild GFAP-astrocytic hypertrophy (arrow). **E:** There was no evidence of a change in the distribution of astrocytes labeled with S100β after acute fenestration with the knife. **F:** Astrocytes labeled with S100β. Scale bars = 100 μm in E (applies to A,C,E); in F (applies to B,D,F).

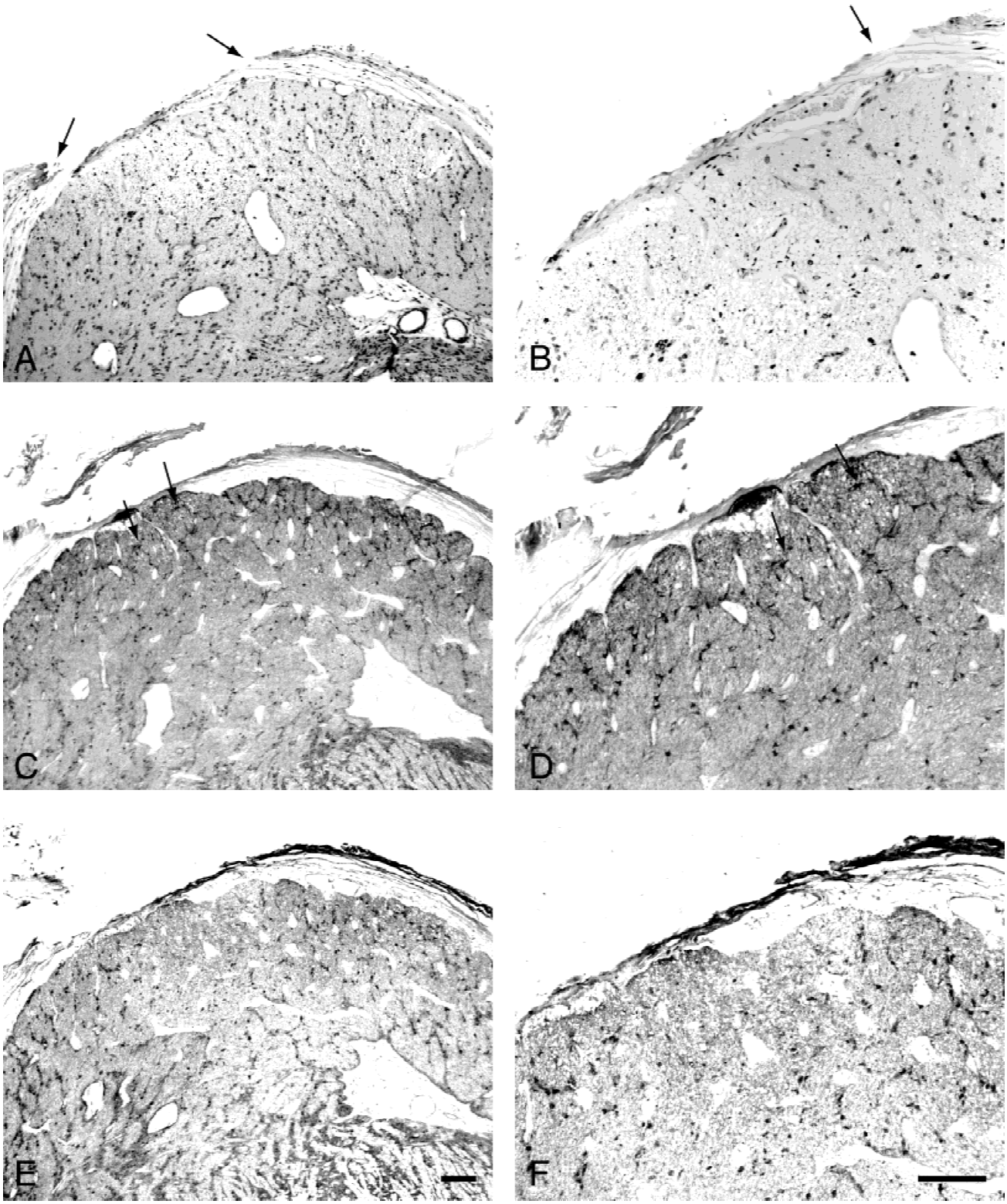

Fig. 6. Illustrated are sections of the optic nerve through the level of the fenestrations produced acutely with the free electron laser (FEL) at 6.45 μm and < 2.5 mJ. The FEL was effective in cutting the sheath. **A:** Edges of the cut sheath were easily observed (arrows; hematoxylin and eosin [H&E]). **B:** Distributions of glia and supporting cells within the nerve were uniform after acute fenestration with the laser (arrow; H&E). **C:** A mild hypertrophy of astrocytes was evident after the acute laser fenestration in glial fibrillary acidic protein (GFAP) -immunoreacted sections, but was limited to a zone adjacent to the fenestration (arrows). **D:** Mild GFAP-astrocytic hypertrophy (arrows). **E:** There was no evidence of a change in the distribution of astrocytes labeled with S100β after acute fenestration with the laser. **F:** Astrocytes labeled with S100β. Scale bars = 100 μm E (applies to A,C,E); in F (applies to B,D,F).

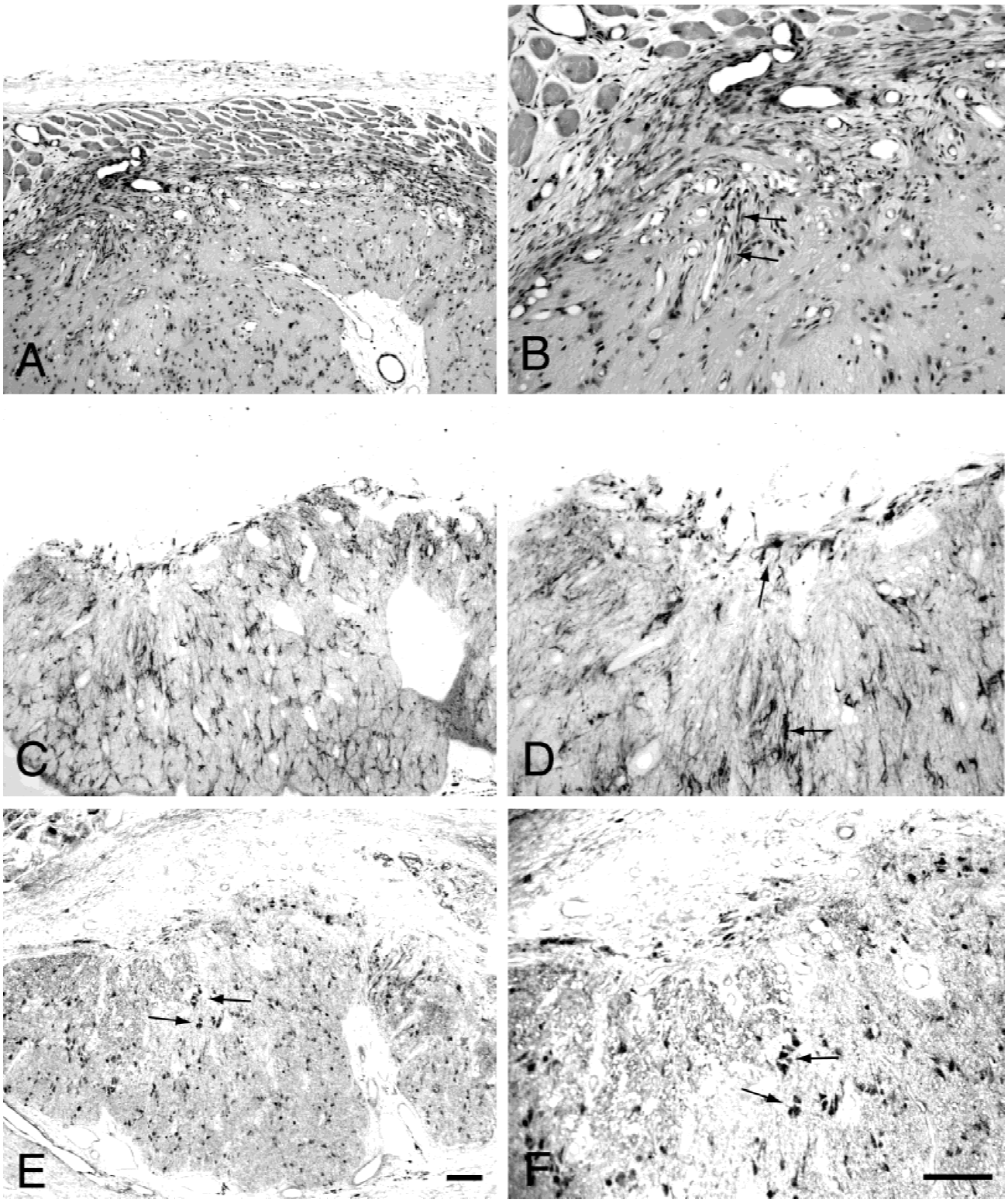

Fig. 7. Damage to the optic nerve only occurred with the free electron laser at an excessive energy level (7.5 mJ) in a rabbit that survived for 1 month. **A:** Damage was evident in the hematoxylin and eosin (H&E) sections through the level of the fenestration. **B:** Fibrous scar tissue covered the damaged portion of the nerve and some fibroblasts appeared to invade the edge of the nerve (arrows; H&E). **C:** Glial fibrillary acidic protein (GFAP) -positive astrocytes were present immediately adjacent to the fenestration and appeared hypertrophied through the full thickness of the nerve. **D:** Hypertrophied astrocytes (arrows, GFAP). **E:** S100β–up-regulated cells were present away from the fenestration site (arrows). **F:** S100β–up-regulated cells were present away from the fenestration site (arrows). Scale bars = 100 μm E (applies to A,C,E); in F (applies to B,D,F).

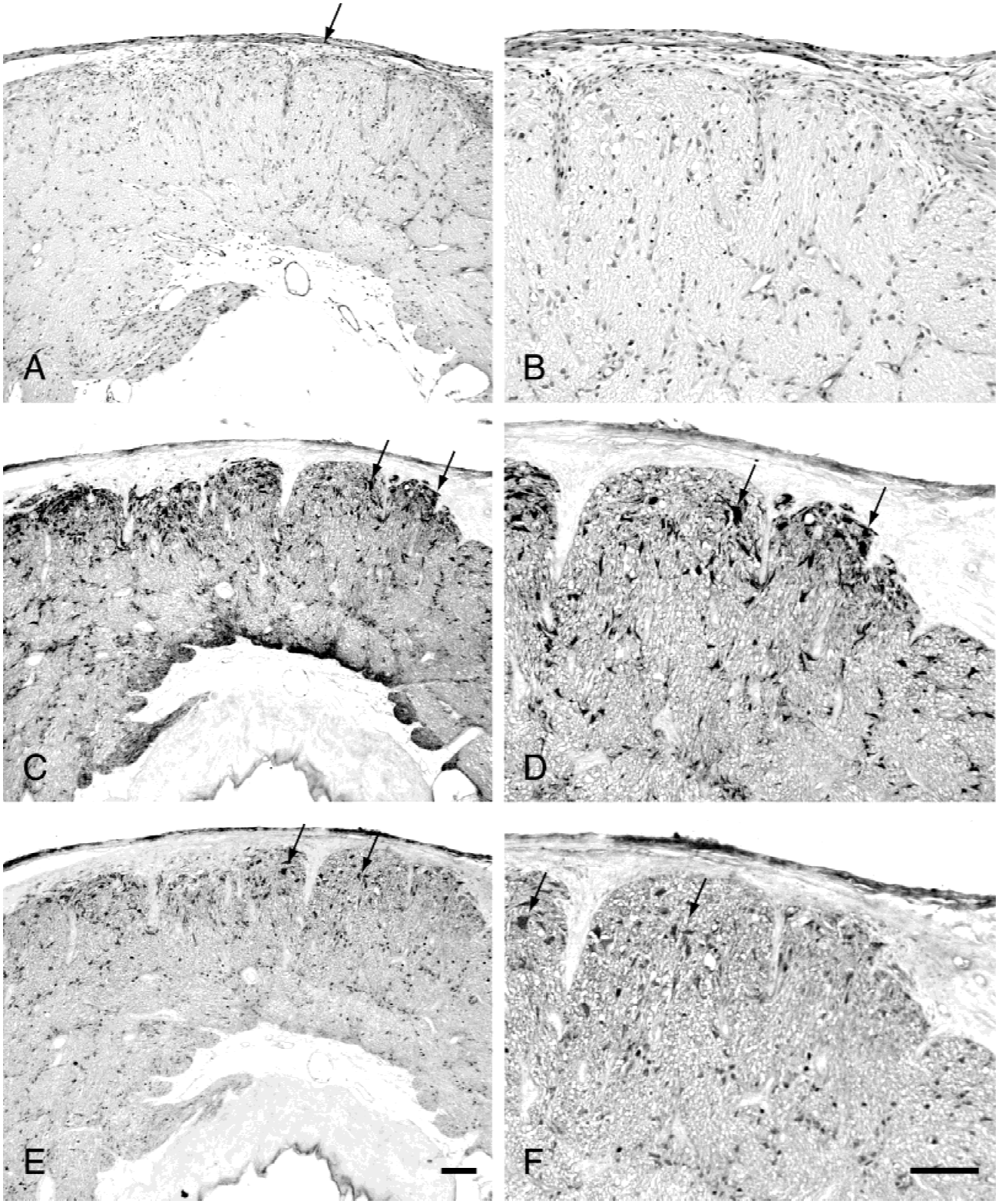

Fig. 8. Healing responses after a knife fenestration after 1-month survival are shown. **A:** A thin fibrous scar was evident at the level of the fenestration completely covering the original opening and extending into the subarachnoid space (arrow). No incision of the optic nerve was observed (hematoxylin and eosin [H&E]). **B:** Glial and supporting cells were evenly distributed (H&E). **C:** Astrocytes appeared hypertrophied in glial fibrillary acidic protein (GFAP) -immunostained sections adjacent to the original site of the fenestration (arrows). **D:** Astrocytes appeared hypertrophied in GFAP-immunostained sections adjacent to the original site of the fenestration (arrows). **E:** Up-regulation of S100β in some glia near the fenestration site was present (arrows). **F:** Up-regulation of S100β in some glia near the fenestration site was present (arrows). Scale bars = 100 μm E (applies to A,C,E); in F (applies to B,D,F).

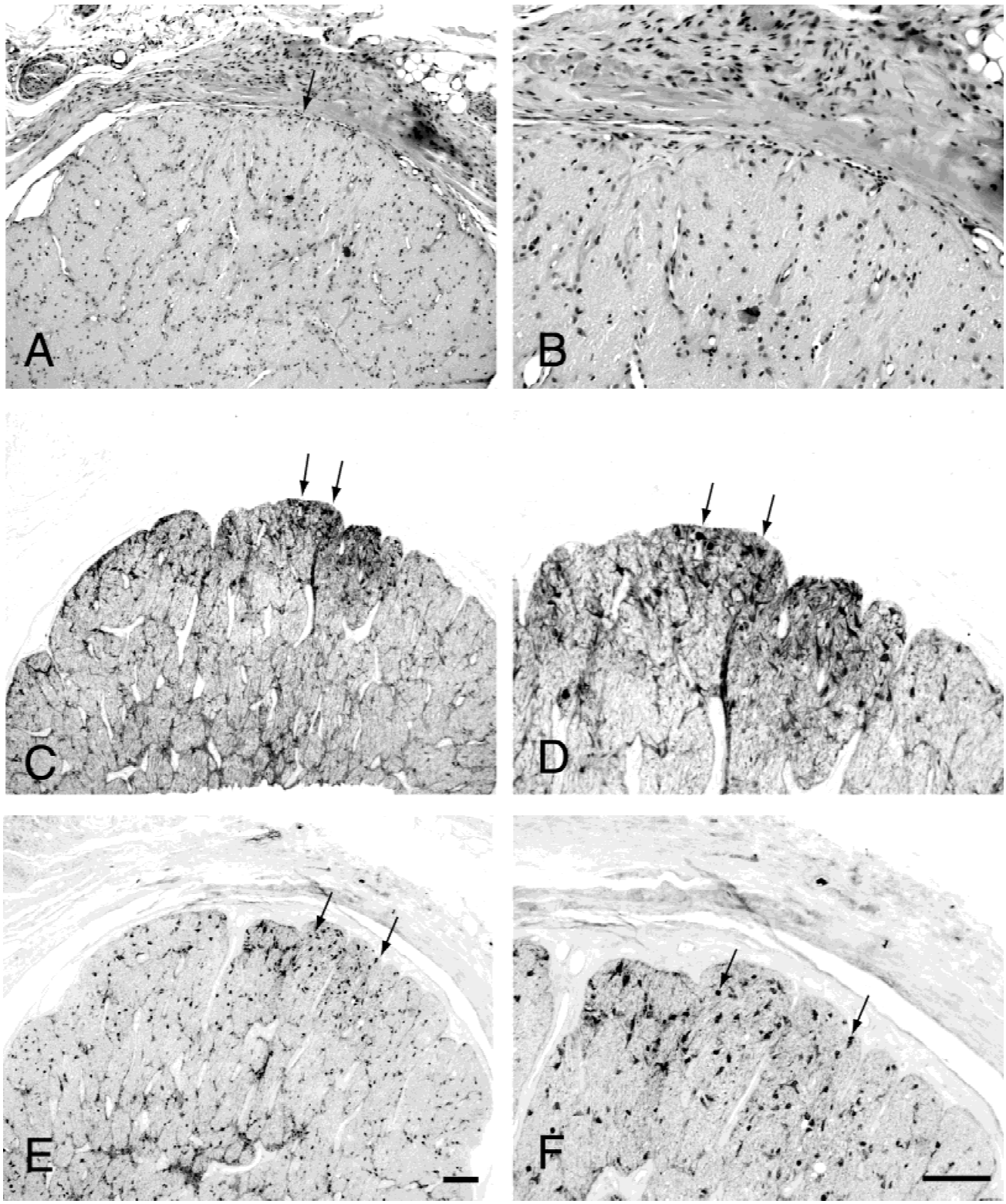

Fig. 9. Healing responses after laser fenestration < 2.5 mJ after 1-month survival are shown. **A:** A thin fibrous scar was evident at the level of the fenestration completely covering the original opening and extending into the subarachnoid space (arrow). No incision of the optic nerve was observed (hematoxylin and eosin [H&E]). **B:** Glial and supporting cells were evenly distributed (H&E). **C:** Astrocytes appeared hypertrophied in glial fibrillary acidic protein (GFAP) -immunostained sections adjacent to the original site of the fenestration (arrows). **D:** Astrocytes appeared hypertrophied in GFAP-immunostained sections adjacent to the original site of the fenestration (arrows). **E:** Up-regulation of S100β in glial cells near the fenestration site was present (arrows). **F:** Up-regulation of S100β in glial cells near the fenestration site was present (arrows). Scale bars = 100 μm E (applies to A,C,E); in F (applies to B,D,F).

macro pulse, and 325-μm spot size is capable of efficiently performing an optic nerve sheath fenestration in a small space. Surgical ease suggests that the FEL is superior to the knife in terms of convenience and control. Both 6.45-μm FEL incisions at < 2.5 mJ and knife incisions result in a similar rapid hypertrophy of astrocytes at the site of fenestration, which remains evident 1 month postoperatively, although the optic nerve appears otherwise undamaged.

Evaluation of the Surgical Approach

We found that the Amide II wavelength produced by the tunable FEL at a relatively low energy <2.5 mJ is adequate for performing the optic nerve sheath fenestration in rabbits. Three times this energy at 7.5 mJ proved too strong with observable tissue damage of the underlying optic nerve. This finding suggests that, as with other forms of laser surgery, precise control of laser parameters is critical for successful outcomes. The infrared FEL energy is propagated through a thin hollow waveguide that has been specially coated to allow energy transmission at this wavelength. The waveguide is enclosed within a surgical probe with a 20-gauge diameter tip and a focusing lens at the end. This arrangement allows maneuverability in small areas such as over the surgically exposed optic nerve sheath. Results of preliminary optic nerve fenestration experiments in monkeys suggest that the FEL also improves surgical ease of this procedure in primates for which the difficulty in visualization of the optic nerve is similar to that in humans [17]. Ideally, one would like to test the usefulness of the FEL in producing a fenestration in animals in which CSF pressure has been elevated with increased fluid volume surrounding the optic nerve. Unfortunately, such models would be difficult to produce under chronic conditions with adequate pain management. However, the surgical procedure should actually be safer and easier to perform under pathologic conditions of increased CSF pressure because the optic nerve would be more protected from an infrared wavelength's effects by the extra surrounding cushion of fluid. The maneuverability of the thin surgical FEL probe also may lead to future advances to reduce the invasive surgical exposure required currently for this procedure.

The Glial Response

Previously, few detailed studies have systematically examined cellular changes and glial responses after optic nerve sheath fenestration. Earlier studies have relied on changes identified by only routine H&E histology [18–21]. In contrast, the normal optic nerve has been studied extensively in a variety of species as a model to understand the cell biology of glia [22–24]. Here we show that, in rabbits, GFAP is up-regulated rapidly within astrocytes in response to limited removal of the nerve sheath. The glial response is localized to the site of the fenestration and does not differ between nerves in which the fenestration is produced with the knife versus the FEL at 6.45 μm at < 2.5 mJ. The acute phase of GFAP up-regulation does not appear to be accompanied by a similar rapid up-regulation of the calcium binding protein S100β, known to be a reliable marker for astrocytes [24,25]. However, after 1-month survival, up-regulation of S100β is observed in a subpopulation of astrocytes adjacent to the fenestration site produced by either the knife or the FEL. This finding suggests that the glial response to the optic nerve sheath fenestration involves at least two phases, i.e., an early phase when astrocytes hypertrophy and a later phase in which some astrocytes up-regulate S100β. It is noteworthy that mild local up-regulation of GFAP but not S100β was also seen in all five sham-operated nerves 1 month postoperatively. The histologic glial response was observed only on the exposed side of the sham surgeries, suggesting that optic nerve astrocytes are very sensitive to minimal manipulation of the optic nerve sheath and can exhibit changes at least 1 month postoperatively. This result indicates that glia can respond to mechanical stimuli, although our data do not address this possibility directly. In the future, it will be useful to examine more carefully the degree to which minimal manipulations of the optic nerve itself are capable of producing a glial reaction and whether such a reaction resolves with time.

Three groups have examined the postmortem appearance of the optic nerve after optic nerve sheath fenestrations in humans. Histology of patients surviving 3 weeks to 3 months after a 6- to 8-mm linear incision of the lateral optic nerve sheath to reduce papilledema demonstrated granulation tissue at the site [19]. Histologic examination of an optic nerve with H&E 39 days after bilateral inferonasal 3 to 5 mm optic nerve sheath slits, performed for chronic papilledema caused by glioblastome multiforme, demonstrated a patent fistula with formed subarachnoid space containing loose connective and arachnoid tissue [20]. In contrast, histopathologic examination of

bilateral optic nerve sheath fenestrations performed for pseudotumor cerebri 14 days before death (unrelated to the fenestration) showed fibroblasts and localized proliferation of connective tissue at the site of the original fenestration [21]. In this patient, visual recovery and resolution of headaches continued after the fenestration until death, suggesting that the surgery was still therapeutically beneficial despite this connective tissue proliferation at the fenestration site. These histologic changes are similar to those observed in the 1-month survival rabbits in our study. Likewise, in an experimental study of optic nerve fenestration by using a knife in nine monkeys with induced papilledema, connective tissue cells bridged the fenestration and often obliterated the subarachnoid space under the incision [18]. These cells also were observed to invade the underlying optic nerve in two cases [18]. The type of healing response and the degree to which the scar blocks CSF outflow may partially explain the variability in the long-term success with optic nerve sheath fenestration.

The FEL at 6.45 μm and low energy (< 2.5 mJ) has shown promise in its ability to successfully incise the optic nerve sheath in rabbits without cutting the underlying optic nerve. Further studies are under way to evaluate this technique in a primate optic nerve model where the anatomic position and sheath are more similar to that in human optic nerves [17]. If the FEL is again found equivalent to or better than standard mechanical optic nerve sheath fenestration methods, then the FEL's advantage of requiring only a thin delivery probe can be explored further. Perhaps the extensive and invasive surgical exposure currently required for optic nerve sheath fenestration could be reduced, especially if the laser probe could be combined with an orbital endoscope for improved visualization.

Recently, a 0.9-mm-diameter endoscope has been successfully combined with a thin glass-hollow waveguide to perform intraocular endoscopic goniotomy with the FEL in congenital glaucoma rabbits with edematous corneas. This FEL surgery successfully lowered the postoperative intraocular pressure for 3 weeks and was comparable to endoscopic goniotomy performed with the standard goniotomy needle [26].

Other surgical fields also have successfully used the FEL. Recently, a neurosurgeon biopsied a small portion of a patient's benign brain tumor with FEL energy at 6.45 μm (M. Copeland, personal communication). A dermatology team has determined that FEL at wavelengths 7.2–7.4 μm and 7.6–7.7 μm may be more efficient than the clinical CO_2 laser in producing cutaneous contraction [27]. The FEL at 6.1 μm to 6.45 μm has been found to efficiently cut cortical bone with less collateral thermal damage than a surgical bone saw [28]. Additional studies are required in these and other areas to fully explore the vast potential of the FEL. In the future, it also will be significant to determine whether laser physicists and engineers can develop a smaller "table-top" FEL, or economical lasers that can produce single wavelengths such as 6.45 μm at clinically useful energies and powers. Such developments will be necessary before useful experimental surgery at these wavelengths can be incorporated into clinical practice.

ACKNOWLEDGMENTS

The authors thank Steve Head, Julia Mavity-Hudson, Amy Nunnally, Richard Robinson, Steve Head, Tony Adkins, Mike Slowey, and the staff at the Vanderbilt Keck Free Electron Laser Facility for their valuable technical assistance.

REFERENCES

1. Ahlskog JE, O'Neill BP. Pseudotumor cerebri. Ann Intern Med 1982;97:249–256.
2. Marcelis J, Silberstein SD. Idiopathic intracranial hypertension without papilledema. Arch Neurol 1991;48:392–399.
3. Lam BL, Schatz NJ, Glaser JS, Bowen BC. Pseudotumor cerebri from cranial venous obstruction. Ophthalmology 1992;99:706–712.
4. Karahalios DG, Rekate HL, Khayata MH, Apostolides PJ. Elevated intracranial venous pressure as a universal mechanism in pseudotumor cerebri of varying etiologies. Neurology 1996;46:198–202.
5. Hayreh MS, Hayreh SS. Optic disc edema in raised intracranial pressure. I. Evolution and resolution. Arch Ophthalmol 1977;95:1237–1244.
6. Corbett JJ, Thompson HS. The rational management of idiopathic intracranial hypertension. Arch Neurol 1989; 46:1049–1051.
7. Corbett JJ, Nerad JA, Tse DT, Anderson RL. Results of optic nerve sheath fenestration for pseudotumor cerebri: the lateral approach. Arch Ophthalmol 1988;106:1391–1397.
8. Spoor TC, McHenry JG. Long-term effectiveness of optic nerve sheath decompression for pseudotumor cerebri. Arch Ophthalmol 1993;111:632–635.
9. Wall M, Dollar JD, Sadun AA, Kardon R. Idiopathic intracranial hypertension: lack of histologic evidence for cerebral edema. Arch Neurol 1995;52:141–145.

10. Spoor TC, McHenry JG, Shin DH. Long-term results using adjunctive mitomycin C in optic nerve sheath decompression for pseudotumor cerebri. Ophthalmology 1995; 102:2024–2028.
11. Mietz H, Prager TC, Schweitzer C, Patrinely J, Valenzuela JR, Font RL. Effect of mitomycin C on the optic nerve in rabbits. Br J Ophthalmol 1997;81:584–589.
12. Joos K, Shen J, Edwards G, Shetlar D, Khoury J, Robinson R. Infrared free electron laser-tissue interactions with human ocular tissues. Invest Ophthalmol Vis Sci 1996;37:S431.
13. Chedid MK, Handy FF, Wilkinson DA, Kennerdell JS, Maroon JC. Temperature distributions in porcine orbital tissues following the use of CO_2 and Nd:YAG lasers. Ophthal Surg 1993;24:100–104.
14. Edwards G, Logan R, Copeland M, Reinish L, Davidson J, Johnson B, Macionas R, Mendenhall M, Ossoff R, Tribble J, Werkhaven J, O'Day, D. Tissue ablation by a free-electron laser tuned to the amide II band. Nature 1994; 371:416–419.
15. Shen JH, Joos KJ, Shetlar DJ, Robinson RD, O'Day DM, Edwards GS. Investigation of a clinical intraocular microsurgical device using the infrared free electron laser. Invest Ophthalmol Vis Sci 1997;38:S86.
16. Hamel LM, Tse DT, Glaser JS, Byrne SF, Schatz NJ. Neuroimaging of the optic nerve after fenestration for management of pseudotumor cerebri. Arch Ophthalmol 1992;110:636–639.
17. Casagrande VA, Joos KM, Shetlar DJ, Powers MK, Shen JH. Chronic and acute optic nerve sheath fenestration in monkeys using the Free Electron Laser (FEL). Invest Ophthalmol Vis Sci 1999;40:S857.
18. Hayreh SS. Pathogenesis of oedema of the optic disc. Doc Ophthalmol 1968;24:289–411.
19. Davidson SI. A surgical approach to plerocephalic disc oedema. Trans Ophthalmol Soc UK 1970;89:669–690.
20. Keltner JL, Albert DM, Lubow M, Fritsch E, Davey LM. Optic nerve decompression, a clinical pathological study. Arch Ophthalmol 1977;95:97–104.
21. Tsai JC, Petrovich MS, Sadun AA. Histopathological and ultrastructural examination of optic nerve sheath decompression. Br J Ophthalmol 1995;79:182–185.
22. Skoff RP, Price DL, Stocks A. Electron microscopic autoradiographic studies of gliogenesis in rat optic nerve: II. Time of origin. J Comp Neurol 1976;169:313–334.
23. Raff MC. Glial cell diversification in the rat optic nerve. Science 1989;243:1450–1455.
24. Zhang MZ, McKanna JA. Gliogenesis in postnatal rat optic nerve: LC1+ microglia and S100β+ astrocytes. Dev Brain Res 1997;101:27–36.
25. Ridet JL, Privat A, Malhotra SK, Gage FH. Reactive astrocytes: cellular and molecular cues to biological function. Trends Neurosci 1997;20:570–577.
26. Sun W, Shen JH, Shetlar DJ, Joos KM. Endoscopic goniotomy with the free electron laser in congenital glaucoma rabbits. J Glaucoma (in press).
27. Ellis DL, Weisberg NK, Chen JS, Stricklin GP, Reinisch L. Free electron laser infrared wavelength specificity for cutaneous contraction. Lasers Surg Med 1999;25:1–7.
28. Peavy GM, Reinisch L, Payne JT, Venugopalan V. Comparison of cortical bone ablations by using infrared laser wavelengths 2.9 to 9.2 μm. Lasers Surg Med 1999;25: 421–434.